Supporting Online Material for

Repulsion of Superinfecting Virions: A Mechanism for Rapid Virus Spread

Virginie Doceul, Michael Hollinshead, Lonneke van der Linden, Geoffrey L. Smith*

*To whom correspondence should be addressed. E-mail: geoffrey.l.smith@imperial.ac.uk

Published 21 January 2010 on *Science* Express
DOI: 10.1126/science.1183173

This PDF file includes:

Other Supporting Online Material for this manuscript includes the following:
(available at www.sciencemag.org/cgi/content/full/science.1183173/DC1)

Supporting online materials

Material and Methods

Viruses and infection. VACV strain Western Reserve (WR) (*S1*) and the deletion mutants vΔA33R (*S2*), vΔA34R (*S3*), vΔA36R (*S4*), vΔAB5R (*S5*), vΔA56R (*S6*), vΔF12L (*S7*), vΔF13L (*S8*), vEGFPA5L (*S9*) and vΔA36R-EGFPA5L (*S10*) were described previously. vΔA33R-EGFPA5L was constructed using vΔA33R (*S2*) and pEGFPA5L (*S9*) by transient dominant selection as described (*S10*). Cells were infected with the different VACVs, overlaid with semi-solid medium containing 1.5% carboxymethylcellulose.

Generation of recombinant VACV viruses and plaque assay. DNA coding for A33, A36 and B5 was introduced into the *Bam*HI/*Eco*RI, *Bam*HI or *Kpn*I restriction sites, respectively, of pRK19, a plasmid containing the VACV 4b late promoter inserted within the VACV thymidine kinase gene. The resultant plasmids were transfected into infected cells to introduce the 4b-*A33R*, 4b-*A36R* or 4b-*B5R* genes into the TK locus of vΔA33R (*S2*) or vΔA33R-EGFPA5L, vΔA36R (*S4*) or vΔA36R-EGFPA5L and vΔAB5R (*S5*), respectively. The resulting viruses, v4b-A33, v4b-A33-EGFPA5L, v4b-A36, v4b-A36-EGFPA5L and v4b-B5, were selected by plaque size and several rounds of plaque purification. The fidelity and purity of the final recombinant virus was confirmed by PCR and cytosine arabinoside (AraC) treatment (Fig. S4) as described (*S4*). For plaque assays, BSC-1 cells were infected for three days and processed as described (*S11*). The radius of 11-12 plaques was determined in three independent experiments using the AxioVision Rel. 4.6 software (Zeiss). The relative plaque size is presented as the percentage of the plaque size obtained with WR or vEGFPA5L.

Generation of cherryFP-actin cells. DNA coding for EGFP was removed from pEYFP-Actin (BD Biosciences) using *Nhe*I and *Bsr*GI and replaced by DNA coding for CherryFP to generate pCherryFP-Actin. Following the transfection of BSC-1 cells and G418 selection, CherryFP-actin was detected by fluorescence microscopy.

Live cell imaging, immunofluorescence and electron microscopy. For live cell imaging, BSC-1 cells were infected and overlaid with semi-solid medium containing 1.5% carboxymethylcellulose to prevent lateral diffusion of virions. Imaging was performed at 37 ºC using a Zeiss Axiovert 200M microscope with a 10x lens and an AxioCam camera (Zeiss). The formation of individual plaques was recorded every h for 12-19 h. The radius of plaque was determined for each time point using AxioVision Rel. 4.6 software (Zeiss). Six to eleven plaques were recorded for each virus and the speed of plaque formation was determined in μm per h using linear regression. For time-lapse confocal imaging, cells were infected with vEGFPA5L and transferred to a microscope stage preheated to 37 °C. Images were acquired every h for 16 h using a Zeiss 510 Meta confocal microscope using Zeiss time-lapse software. For immunostaining, coverslips were seeded with cells and fixed with 4% or 8% paraformaldehyde in 250 mM HEPES (pH 7.4) in PBS. The cells were permeabilized with Triton-X-100 (VWR) when required, blocked in 0.5% BSA or 10% FBS and incubated with a mouse anti-v5 mAb (AbD

Serotec), a rabbit polyclonal Ab raised against the cytoplasmic domain of A33 (*S12*), a rat mAb anti-B5 19C2 (*S13*) or mouse mAbs directed against A34 (34-1) and A36 (6.3) (*S14*). A mouse mAb directed against ARPC5 was used to detect the Arp2/3 complex (p16-Arc, clone 323H3, Synaptic system). Secondary Alexa 546-conjugated donkey anti-mouse or rabbit Abs were used to detect bound primary Ab. Alexa 546-conjugated phalloidin (Molecular Probes) was used to stain actin. Samples were mounted in Mowiol–4',6-diamidino-2-phenylindole (DAPI) mounting medium. Microscopy was carried out with a Zeiss 510 Meta confocal microscope (Zeiss).

For electron microscopy, samples were labelled with mouse anti-v5 mAb, followed by secondary horseradish peroxidase conjugated anti-mouse Ab, and reacted with DAB / Metal (Pierce) for 30 min. Samples were viewed by widefield microscopy Zeiss Axiovert 200M and then embedded in Epon. Sections were stained with Reynold's lead citrate and viewed using an FEI Tecnai G2 electron microscope (FEI, Eindhoven, The Netherlands) with a Soft Imaging System Megaview III charge-coupled device camera. Images were collected using ANALYSIS version DOCU software (Olympus Soft Imaging Solutions, Münster, Germany).

Generation of HeLa cells expressing VACV proteins. DNA fragments corresponding to *A33R* or *A36R* were amplified from pcDNA3-A33 and pcDNA3-A36, two plasmids derived from pcDNA3 (Invitrogen) containing the VACV WR *A33R* and *A36R* genes, and cloned into the *Bam*HI or *Mlu*I/*Bam*HI sites of the lentivirus vector pdlNot'MCS'R'PK derived from pHR-SIN-CSGW (*S15*). A control lentivirus (v5) and lentiviruses expressing A33- v5 and A36-v5 were produced as described (*S15*). HeLa cells were infected with the different lentiviruses and cells were selected using puromycin. A clonal cell line expressing A33-v5 was produced subsequently to optimise A33 expression and this was transduced with lentiviruses expressing A36-v5 to create the HeLa cells A33-v5/A36- v5.

Preparation of fresh EEVs, spinoculation and actin tails. Fresh EEVs from the supernatant of vEGFPA5L-infected cells were clarified by centrifugation for 10 min at 1000 *g* at 4 °C and spinoculated onto chilled HeLa cells, or derivative cells expressing A33-v5, A36-v5 or both proteins, at 650 *g* for 30 min at 4 °C. The cells were overlaid with warm medium and incubated for 15 or 30 min at 37 °C. The samples were then fixed in 4% PFA and stained for actin and B5. Actin tails were counted on the entire surface of three independent coverslips (24-mm diameter) for each cell line. A33-v5/A36- v5 HeLa cells were also spinoculated with fresh EEVs (vEGFPA5L), purified IMVs (vEGFPA5L) and virions from a recombinant HSV-1, 166v, expressing GFP-tagged VP-22 (*S16*). The mean number of virions bound per cell were determined as 27.66 ± 2.072, 22.50 ± 2.88 or 28.78 ± 5.20 for EEVs, IMVs and HSV-1 respectively (SEM, mean from 3 independent experiments with n=5 fields of 4 to 12 cells), indicating the failure to induce actin tails with IMV and HSV-1 was not due to lack of virus binding.

Preparation of cell lysates and immunoblotting. Cells were washed with PBS and lysed in RIPA buffer (25 mM Tris HCl pH 8.8, 50 mM NaCl, 0.5% Nonidet P-40 and 0.1% sodium dodecyl sulphate). Insoluble material was centrifuged at 16 000 *g* for 20

min. Immunoblot analysis of cell lysates was performed using the primary mouse anti-v5 mAb (AbD serotec), a mouse anti-A33 mAb (A33-1), a rabbit polyclonal anti-A36 Ab (*S12*), the rat anti-B5 mAb 19C2 (*S13*), a rabbit polyclonal Ab raised against K7, an anti-D8 mAb (AB1.1 (*S4*)) and a mouse anti-α-tubulin mAb (clone DM1A, Millipore). The secondary Abs used were goat anti-rabbit, anti-mouse (Stratech Scientific) and anti-rat-horseradish peroxidase (GE Healthcare).

Statistical analysis. The data in the graphs are represented as mean and standard error of the mean.

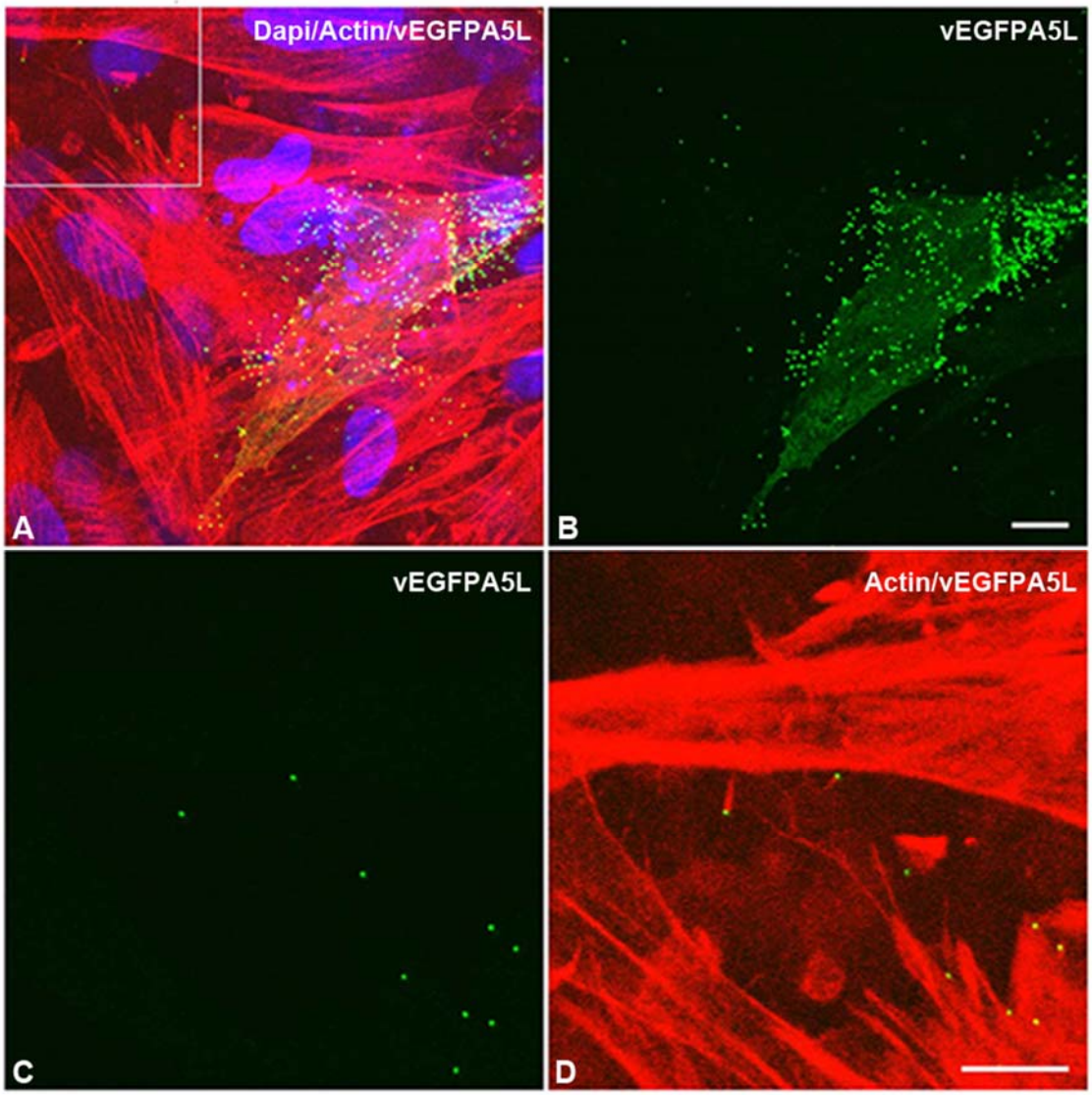

Fig. S1. Spread of VACV in chick embryo fibroblasts (CEFs). CEFs were infected with vEGFPA5L at low multiplicity of infection (moi) and stained with DAPI and phalloidin, and analysed by confocal microscopy. (**A**) Merge of DAPI, phalloidin and EGFP fluorescence images. (**B**) EGFP fluorescence image showing infected cell producing new virions and spread of virions to distant cells. (**C** and **D**) The lower panels show a zoomed image of the area indicated by a white box (**A**) where an actin tail is present on a cell with no virus factory. Panel C shows the EGFP fluorescence showing individual virions. Panel D shows the merge of EGFP and actin staining. Scale bar, 10 μm.

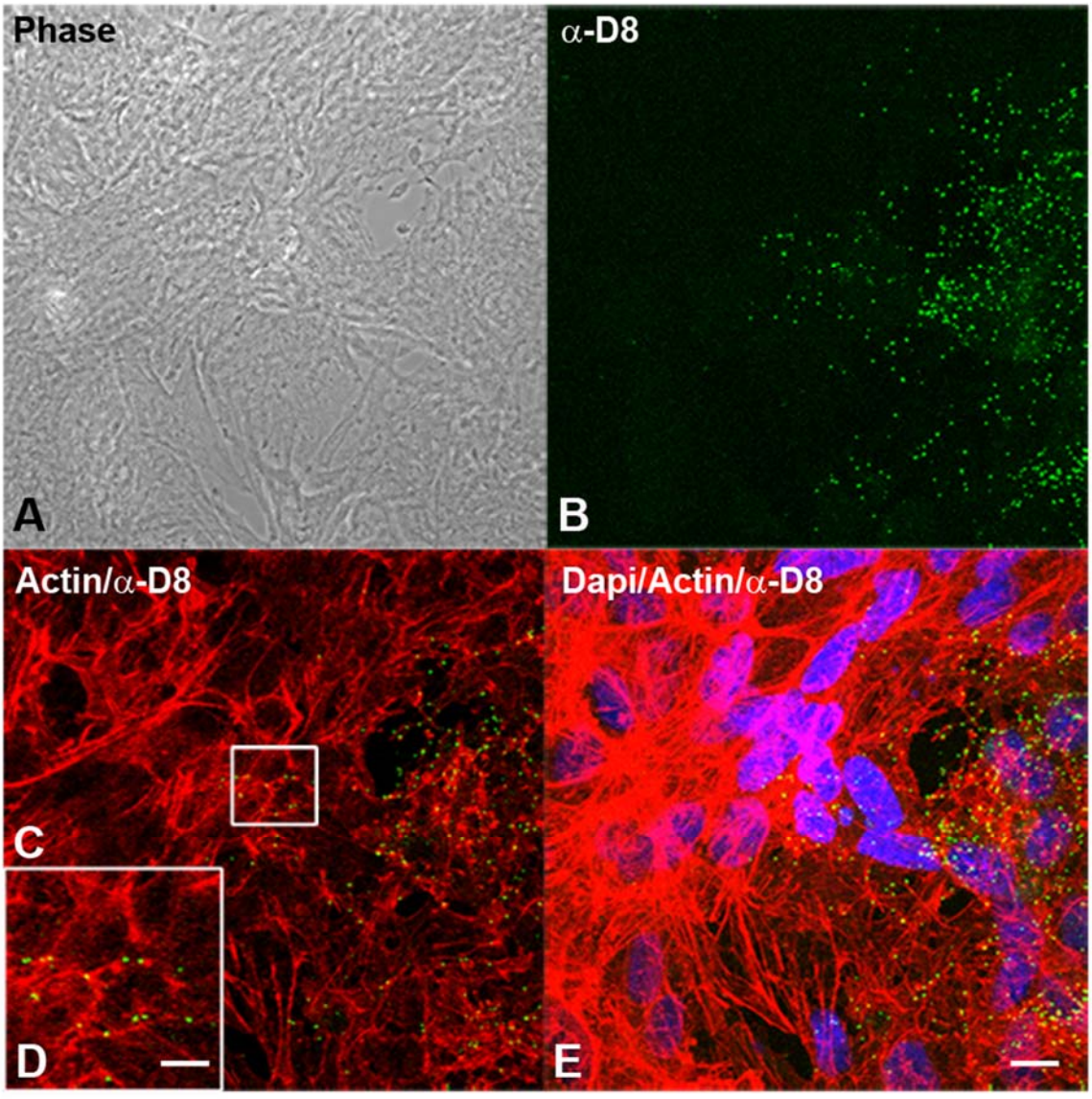

Fig. S2. Spread of VACV strain Lister. BSC-1 cells were infected with VACV strain Lister at low moi and processed for confocal microscopy. Cells were fixed and permeabilized and virus particles were stained with anti-D8 mAb AB1.1 (green), actin

was stained with phalloidin (red) and DNA was stained with DAPI. Confocal microscopy was used to record the edge of a plaque by phase (**A**) and D8 immunofluorescence (**B**). A zoomed image (**D**) of an area at the edge of the plaque indicated by a white box (**C**) shows the presence of an actin tail in a cell with no virus factory. (**E**) Merged image. Scale bar, 10 μm, (**A** to **C**, **E**) and 5 μm (**D**).

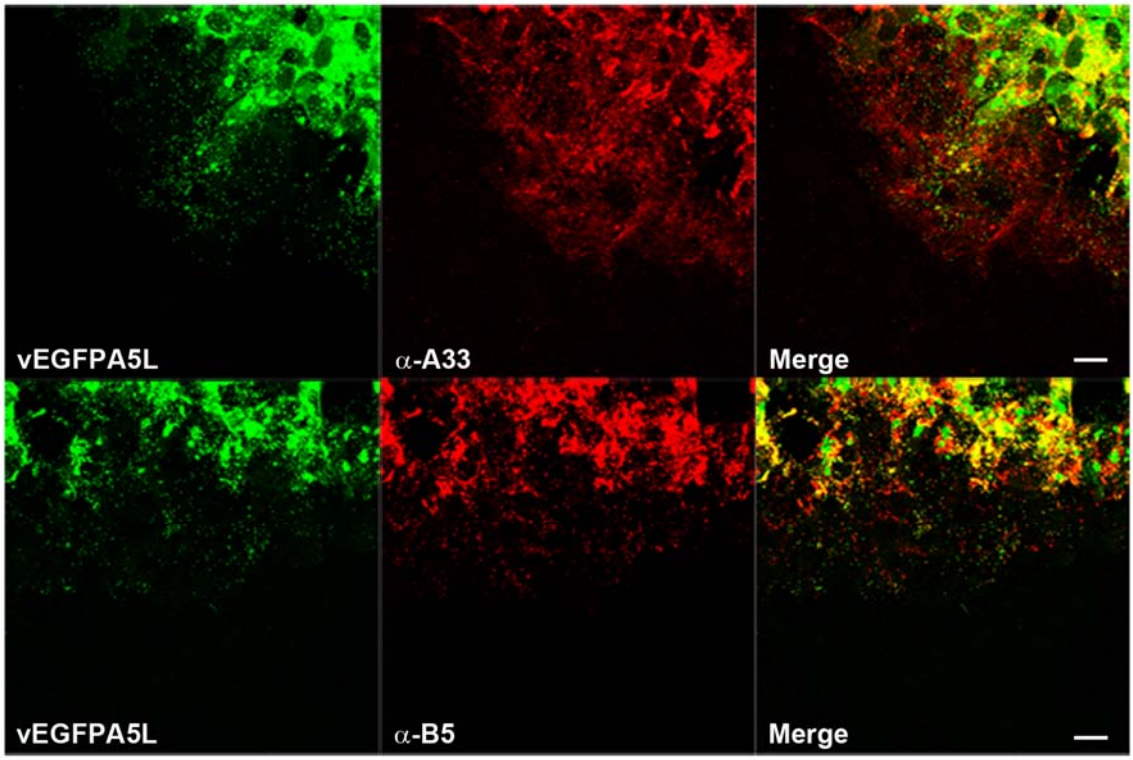

Fig. S3. A33 is expressed early during infection before EGFPA5L. BSC-1 cells were infected with vEGFPA5L at low moi and subsequently the edge of a plaque was visualised by confocal microscopy and immunostaining with anti-A33 (mouse mAb, top row) or anti-B5 (rat mAb, bottom row). The left panel of each row shows the EGFP fluorescence, and the right panel shows the merged image of the left 2 panels. Note the distribution of EGFP and B5 on cells is similar, whereas the A36 stain extends further than the EGFP positive cells, indicating early expression. Scale bar, 20 μm.

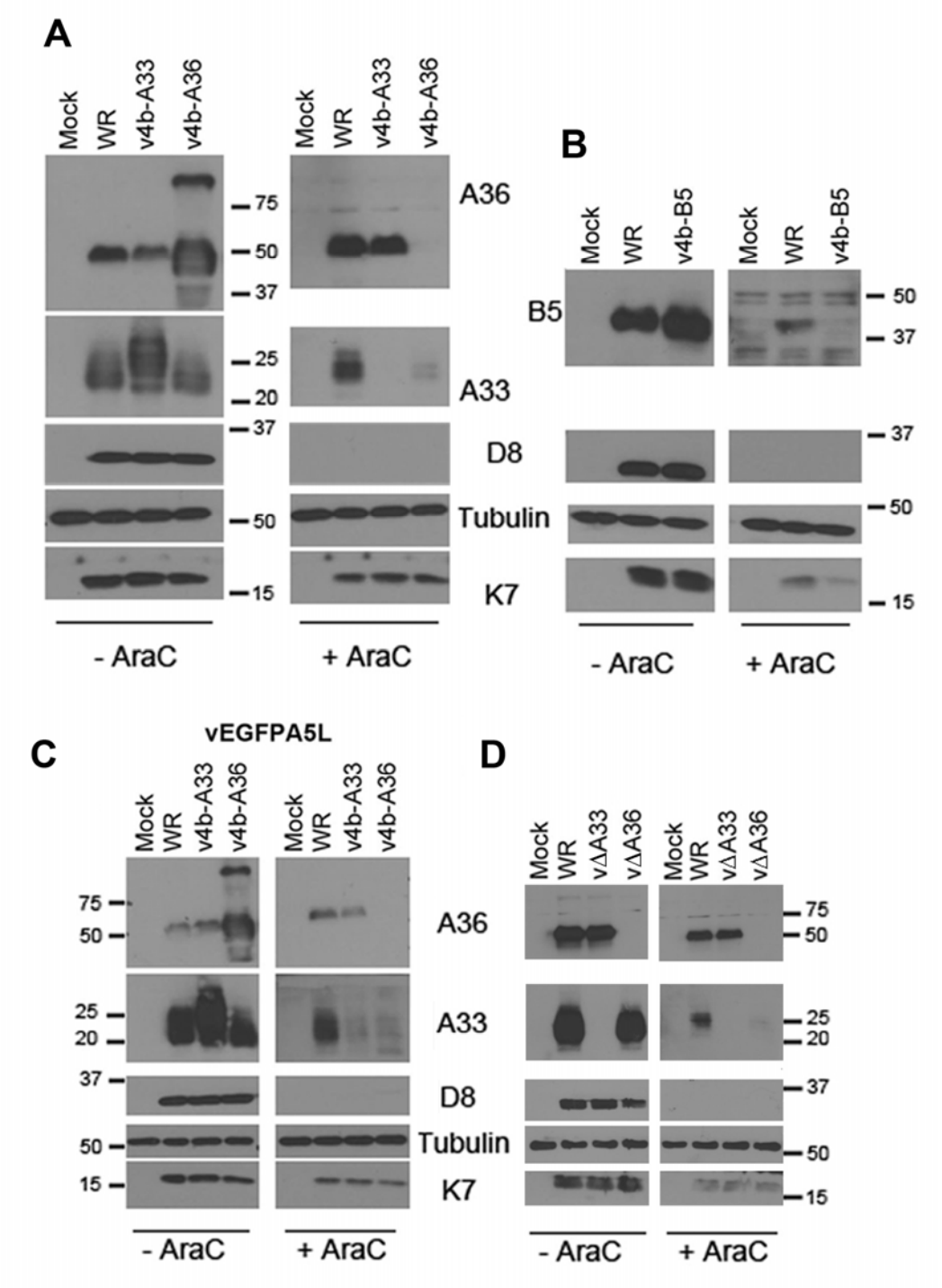

Fig. S4. Immunoblot analysis showing that A33, A36 or B5 are made late during infection when these proteins are expressed from the VACV 4b promoter. BSC-1 cells were either mock-infected or infected with VACV WR (**A** to **C**), v4b-A33R and v4b-A36R (**A**), v4b-B5R (**B**) and v4b-A33R-EGFPA5L and v4b-A36R-EGFPA5L (**C**) at 5

pfu/cell for 24 h in the presence or absence of cytosine arabinoside (AraC, 40 μg/ml). Cell lysates were analyzed by SDS-PAGE and immunoblotting with Abs to VACV proteins A33, A36, B5, D8 and K7 or to alpha tubulin. The images showing expression of A33, A36 and B5 in the presence of AraC were obtained after longer exposure of the X-ray films in comparison to other samples. Note that early during infection, in the absence of A36, A33 is present at lower levels. The same observation was made in cells infected with vΔA36 in comparison to WR (**D**). The level of A33 is also higher in the cells expressing both A33-v5 and A36-v5 in comparison to the parental cell line expressing A33-v5 alone (Fig. 4A).

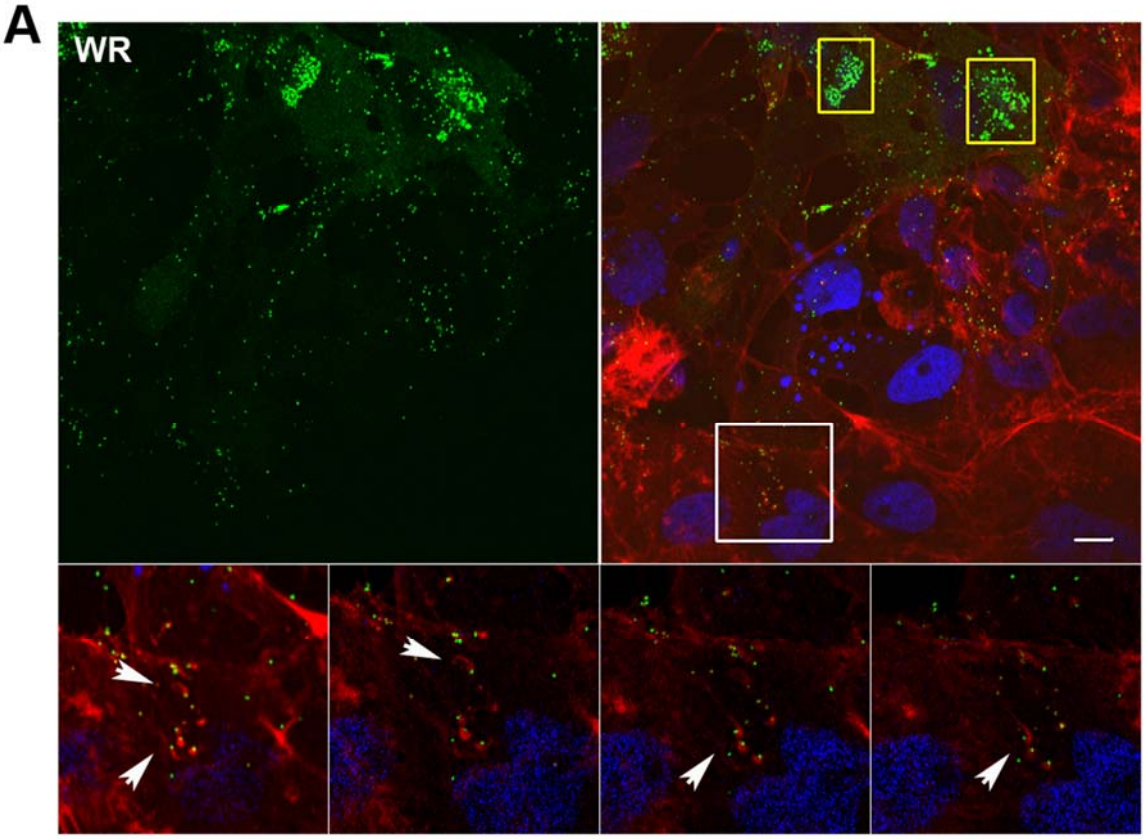
A
WR

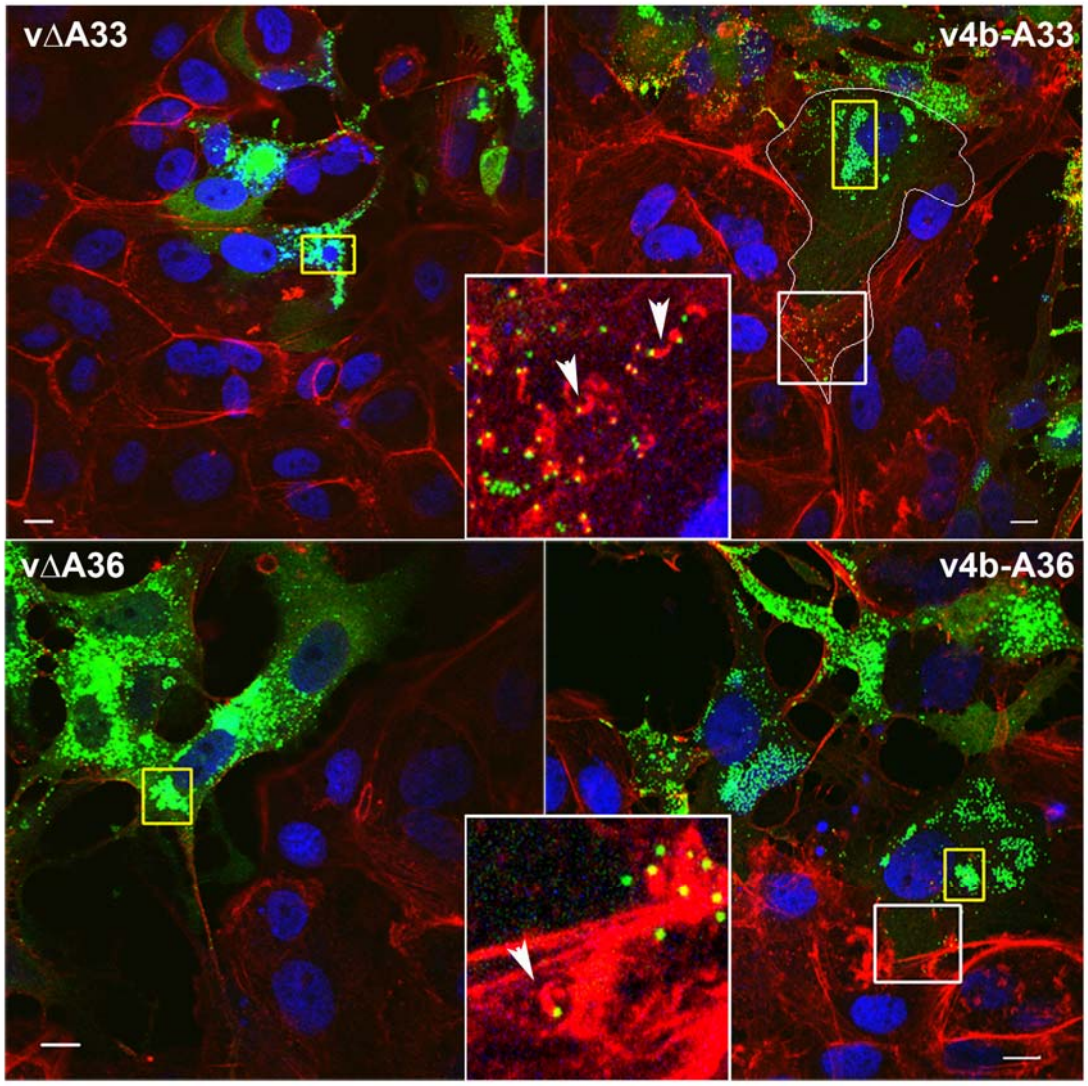
B
vΔA33
v4b-A33
vΔA36
v4b-A36

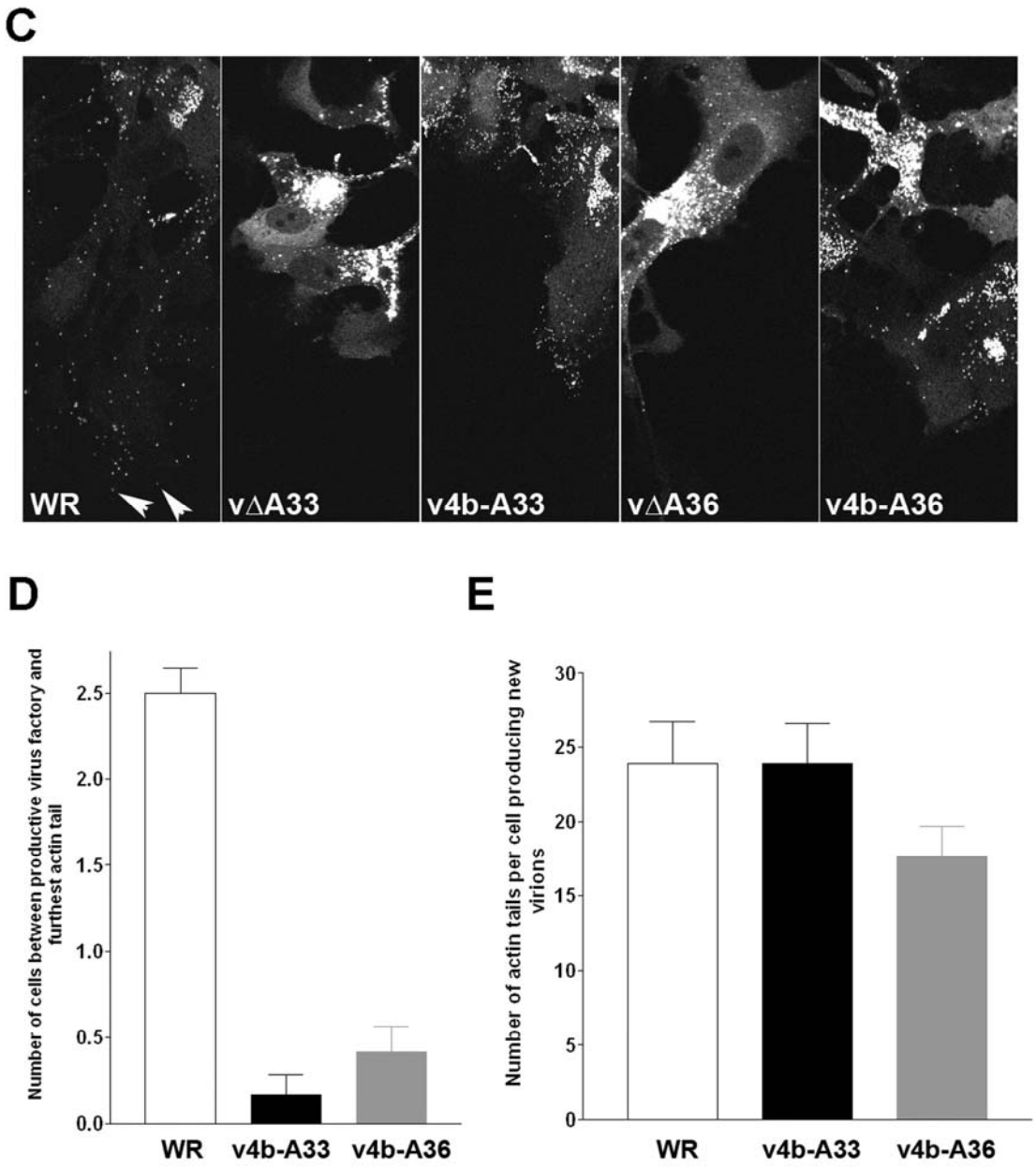

Fig. S5. Confocal microscopy showing early expression of A33 and A36 is needed for efficient spread of VACV particles. (**A**) Images (single focal plane) showing the edge of plaques formed by vEGFPA5L WR (green, upper left panel) stained with phalloidin (red) and Dapi (blue, upper right panel). Virus particles (green) on red actin tails (white box) were detected 2 to 3 cells away from the cell containing green virus factories (yellow box). Lower panel represents 4 different focal plans of the white box (upper right panel), confirming the presence of red actin tails (white arrows). Scale bar, 10 μm. (**B**) Confocal

images showing the edge of plaques formed by vEGFPA5L viruses (green) expressing A36 and A33 under a late promoter only (v4b-A33 and v4b-A36) and with the deletion mutants (vΔA36 and vΔA33) stained with phalloidin (red) and Dapi (blue). Virus particles (green) on actin tails (white boxes) were detected on cells producing virus factories (yellow boxes) for v4b-A33 and v4b-A36. Insets show zoomed images of these actin tails as indicated by white arrows. No actin tail was detected for vΔA36 and vΔA33. Scale bar, 10 μm. (**C**) The spread of virus particles (white dots) away from the edge of the plaque is considerably reduced following infection with the vEGFPA5L viruses v4b-A33 and v4b-A36 and more drastically with vΔA36 and vΔA33 in comparison to WR (white arrows). The panel shows cropped versions of the images presented in figure S5A and B with vEGFPA5L represented in white for clarity. (**D**) Graph representing the mean number of cells present between productive virus factories and the furthest actin tails detected (n=12). Actin tails were detected 2 to 3 cells away from the closest cells containing green virus factories in plaques formed by vEGFPA5L, whereas actin tails were detected only on cells expressing EGFPA5L or producing new virus particles for vEGFPA5L viruses expressing A33 and A36 under a late promoter only. **(E**) Graph representing the mean number of actin tails present in cells with productive virus factories in plaques formed by vEGFPA5L WR, v4b-A33 and v4b-A36 (n=12).

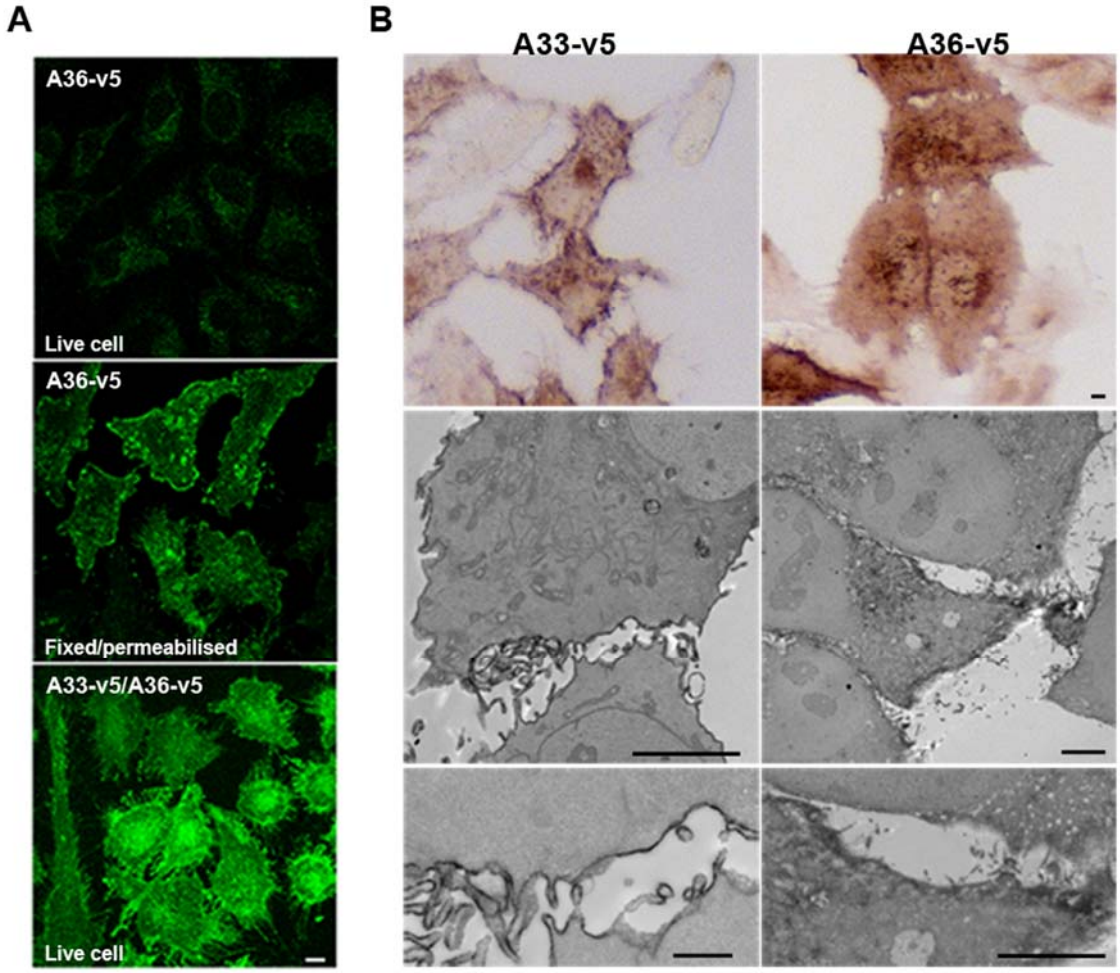

Fig. S6. Immunostaining and electron microscopy images showing that A33-v5 and A36-v5 localise to the cell surface when ectopically expressed in HeLa cells. (**A**) Immunostaining of A36-v5 on HeLa A36-v5 cells either live (top panel) or fixed and permeabilized (middle panel) using an anti-v5 antibody. Note that the v5-specific staining was only detected on fixed and permeabilized HeLa-A36-v5 cells because the v5 tag is fused at the C terminus of A36 that is present in the cytoplasm. In contrast staining of live HeLa A33-v5/A36-v5 cells recognised the v5 tag fused at the C terminus of A33 that is present outside the cell. Scale bar, 10 μm. (**B**) Immunostaining and electron microscopy. The upper panel shows the localization of A33-v5 and A36-v5 using an anti-v5 antibody by immunoperoxidase/DAB staining. The samples were then processed for electron microscopy as shown in the middle and the lower (zoomed image) panels. Scale bar, 5 μm and 1 μm (bottom left panel only).

Movie legends

Movie S1. Movie showing VACV plaque formation. BSC-1 cells were infected with VACV strain WR at low moi and the formation of a plaque was recorded by phase microscopy every h for 16 h after a small plaque first became visible. Note that the motility of infected cells is restricted to within the area showing cytopathic effect (cpe). Virus-induced cell motility is therefore not increasing the rate of spread across the cell monolayer.

Movie S2. Movie showing plaque formation by a VACV strain vEGFPA5L. This virus expresses EGFP fused to the A5 core protein late during infection. BSC-1 cells were infected with vEGFPA5L at low moi and the progression of infection on one side of a plaque was recorded by phase microscopy every h for 16 h.

Movie S3. Movie as for movie 2 except that the growth of the vEGFPA5L plaque was visualized by the EGFP fluorescence.

Movie S4. Movie as for movies 2 and 3 showing merge of phase and fluorescence images. Note that the spread of virus-induced cpe (an early event) precedes that of expression of EGFPA5L, which is made only late during infection.

Movie S5. Movie showing the spread of the edge of a plaque formed by vEGFPA5L at higher rmagnification to show individual virus particles (green dots). Cells were visualised by confocal microscopy using EGFP flourescence. Note cells must express EGFP prior to production of new virus particles and yet there are numerous virus particles on cells distal to those cells expressing EGFP.

Movie S6. Movie showing the formation of actin tails (red) in BSC-1 cells expressing cherryFP-actin that have been infected with vEGFPA5L (green). The movie shows a single focal plane at the periphery of an infected cell where actin tails are formed following the transport of virus particles to the cell periphery (duration, 5 min).

Movie S7. Movie showing green virus particles moving on the tip of red actin tails on a cell expressing cherry-actin and lacking green virus factories. Note that a virus-tipped red actin tail produced by this cell induces the formation of another actin tail after re-contacting the cell surface.

References

S1. A. Alcami, G. L. Smith, *Cell* **71**, 153 (Oct 2, 1992).
S2. R. L. Roper, E. J. Wolffe, A. Weisberg, B. Moss, *J Virol* **72**, 4192 (May, 1998).
S3. A. A. McIntosh, G. L. Smith, *J Virol* **70**, 272 (Jan, 1996).
S4. J. E. Parkinson, G. L. Smith, *Virology* **204**, 376 (Oct, 1994).
S5. M. Engelstad, G. L. Smith, *Virology* **194**, 627 (Jun, 1993).
S6. C. M. Sanderson, F. Frischknecht, M. Way, M. Hollinshead, G. L. Smith, *J Gen Virol* **79 (Pt 6)**, 1415 (Jun, 1998).
S7. W. H. Zhang, D. Wilcock, G. L. Smith, *J Virol* **74**, 11654 (Dec, 2000).

S8. R. Blasco, B. Moss, *J Virol* **66**, 4170 (Jul, 1992).
S9. G. C. Carter *et al.*, *J Gen Virol* **84**, 2443 (Sep, 2003).
S10. E. Herrero-Martinez, K. L. Roberts, M. Hollinshead, G. L. Smith, *J Gen Virol* **86**, 2961 (Nov, 2005).
S11. M. Law, R. Hollinshead, G. L. Smith, *J Gen Virol* **83**, 209 (Jan, 2002).
S12. S. Rottger, F. Frischknecht, I. Reckmann, G. L. Smith, M. Way, *J Virol* **73**, 2863 (Apr, 1999).
S13. M. Schmelz *et al.*, *J Virol* **68**, 130 (Jan, 1994).
S14. H. van Eijl, M. Hollinshead, G. L. Smith, *Virology* **271**, 26 (May 25, 2000).
S15. C. Demaison *et al.*, *Hum Gene Ther* 13, 803 (May 1, 2002).
S16. G. Elliott, P. O'Hare, *J Virol* 73, 4110 (May, 1999).